Wireless Personal Communications **26:** 53–76, 2003.
© 2003 *Kluwer Academic Publishers. Printed in the Netherlands.*

A Decision Aided CDMA Receiver with Partially Adaptive Decorrelating Multi-User Interference Cancellation ⋆

GAU-JOE LIN and TA-SUNG LEE⋆⋆

Department of Communication Engineering and Microelectronics and Information Systems Research Center, National Chiao Tung University, Hsinchu, Taiwan, R.O.C.
E-mail: tslee@mail.nctu.edu.tw

Abstract. A CDMA receiver with enhanced multiple access interference (MAI) suppression is proposed for a pilot symbols assisted system over multipath channels. The design of the receiver involves the following procedure. First, blind adaptive correlators are constructed at different fingers based on the scheme of generalized sidelobe canceller (GSC) to collect the multipath signals and suppress MAI. A low-complexity partially adaptive (PA) realization of the GSC correlators is proposed which incorporates multi-user information for reduced rank processing. By a judiciously designed decorrelating procedure, a new GSC structure is obtained in which the MAI are decorrelated and suppressed individually. The next step is then a simple coherent combining of the correlator outputs with pilot aided channel estimation. Finally, further performance enhancement is achieved by an iterative scheme in which the signal is reconstructed and subtracted from the GSC correlators input data, leading to faster convergence of the receiver. The proposed low-complexity PA CDMA multi-user receiver is shown to be robust to multipath fading and channel errors, and achieve nearly the same performance of the ideal maximum SINR and MMSE receivers by using a small number of pilot symbols.

Keywords: CDMA, multi-user receiver, interference suppression, generalized sidelobe canceller (GSC), partially adaptive GSC (PA GSC).

1. Introduction

The direct sequence CDMA air interface has been selected to be a major candidate for providing multimedia services in the third generation mobile radio communications. However, two major factors in a CDMA system that limit the overall system capacity are the multiple access interference (MAI) and multipath fading. In the worst case, strong MAI causes the near-far problem and severe multipath propagation induces deep fading and/or inter-symbol interference (ISI). In order to successfully detect the data transmitted from the desired user, these interferences need to be suppressed effectively. Adaptive multi-user detectors (MUD) [1] and interference cancellers have been suggested which provide full or partial immunity to the near-far effect [2, 3]. On the other hand, the RAKE receiver is employed as a means of coherent combining of multipath signals by exploiting the temporal signature of the channel. Combination of MUD and RAKE receiver thus offers a feasible solution to the MAI/fading problem.

The linear multi-user detector is an improved version of the conventional RAKE receiver. The improvement lies in its better MAI suppression via either post- or pre-despread processing

⋆ This work was sponsored jointly by the Ministry of Education and National Science Council, R.O.C., under the Contract 89-E-FA06-2-4.
⋆⋆ Corresponding author.

[4]. The post-despread MUD works with the outputs of a bank of filters, each matched to a user of interest. Alternatively, the pre-despread MUD can be regarded as an adaptive matched filter that performs despreading and MAI suppression simultaneously. Popular pre-despread MUDs include the minimum mean squared error (MMSE) [5] and minimum output energy (MOE) receivers [6]. The MMSE receiver minimizes the mean squared error (MSE) between the receiver output and known transmitted symbols. It requires the task of matrix inversion in the batch mode. The MOE receiver derives its filter weights by minimizing the output energy subject to a unit response constraint for the desired signal. It is similar in structure to the linearly constrained minimum variance (LCMV) beamformer in array processing [7], and is shown to offer the performance of the MMSE receiver without the need of channel information [6]. Unfortunately, the MOE receiver exhibits high sensitivity to channel mismatch and does not perform reliably in the presence of multipath propagation. Techniques based on multiple constraints have been proposed to remedy the sensitivity problems [8, 9]. Although the pre-despread CDMA receivers provide excellent MAI suppression, they requires an $(M-1)$-dimensional adaptive processing (typically involving a matrix inversion), where M is the processing gain. To reduce the complexity due to a large M, partially adaptive (PA) realization is suggested as an alternative with which the number of adaptive weights is reduced [10, 11]. The advantages of PA implementation include reduced complexity and faster convergence. However, the performance of interference suppression usually degrades as a result of a smaller processing dimension.

In this paper, a CDMA multi-user receiver with enhanced MAI suppression is proposed for a time-multiplexed pilot symbols assisted system over multipath channels. The design of the receiver involves the following procedure. First, a set of blind adaptive correlators is constructed to collect multipath signals with different delays. The tap weights of each correlator are determined in accordance with the LCMV criterion so that strong MAI can be effectively suppressed. To avoid signal cancellation incurred with channel mismatch, the LCMV correlators are implemented in the form of generalized sidelobe canceller (GSC) [7], and a modified blocking matrix is designed to remove the signal from the received data. For reduced complexity processing, partial adaptivity is incorporated into the GSC correlators. To achieve the optimal MAI suppression, this is done by selecting a reduced dimension subspace of the column space of the blocking matrix representing the MAI signatures obtained in a multi-user scenario. Furthermore, with a judiciously designed decorrelating procedure, a new GSC structure is obtained in which the MAI are decorrelated and suppressed individually such that matrix inversion involved in computing the correlator weight vectors can be avoided entirely, leading to a very low-complexity implementation. Second, a simple coherent RAKE combiner with pilot aided channel estimation gives the desired user's symbol decisions. Since strong interference has been removed, channel estimation can be done accurately with a small number of pilot symbols. Finally, further enhancement in output SINR is achieved by an iterative scheme in which the signal is reconstructed and subtracted from the GSC correlators input data. This effectively eliminates the performance drop due to finite data samples effect, thereby increasing the convergence speed of the receiver. It is shown that the low-complexity PA CDMA multi-user receiver is insensitive to multipath fading and channel estimation errors, and offers nearly the same performance of the ideal maximum SINR (MSINR) and MMSE receivers, which requires a higher complexity and overhead for pilot symbols.

2. Data Model and Linear CDMA Receivers

Consider a CDMA system with K active users. The kth user's contribution to the received signal can be written as

$$r_k(t) = \sqrt{P_k} \sum_i d_k(i) c_k(t - iT) , \tag{1}$$

where P_k denotes the transmit power, $d_k(i)$ denotes the ith transmitted information symbol assumed to be i.i.d. with zero-mean and unit variance, T is the symbol duration. In a time-multiplexed pilot symbols assisted system, a data packet is composed of $N_s = N_p + N_d$ symbols, with the first N_p symbol being pilot symbols $d_{k,p}(i)$, $i = 1, \ldots, N_p$, followed by N_d data symbols, $d_{k,d}(i)$, $i = N_p + 1, \ldots, N_s$. That is (for a single packet),

$$d_k(i) = \begin{cases} d_{k,p}(i), & \text{for } 1 \leq i \leq N_p \\ d_{k,d}(i), & \text{for } N_p + 1 \leq i \leq N_s. \end{cases} \tag{2}$$

In (1), $c_k(t)$ is the signature waveform given by

$$c_k(t) = \sum_{m=0}^{M-1} c_k[m] p(t - mT_c) , \tag{3}$$

where $c_k[m]$ is the spreading sequence of the kth user, M is the spreading factor, $p(t)$ is the chip waveform, and T_c is the chip duration. The transmission channel is modeled as with L resolved Rayleigh fading paths spanning a delay spread of L chips. Putting the K user signals together, the received baseband data can be expressed in the following form:

$$x(t) = \sum_{k=1}^{K} \sum_{l=1}^{L} \alpha_{k,l} r_k(t - \tau_{k,l}) + n(t) , \tag{4}$$

where $\tau_{k,l}$ and $\alpha_{k,l}$ are the delay and complex gain, respectively, of the lth path of the kth user. The $n(t)$ is the additive white noise process with power σ_n^2. For convenience, it is assumed that all CDMA signals have been chip synchronized at the receiver. To fully exploit the temporal signature, $x(t)$ is chip matched filtered and then chip rate sampled at $t = (i-1)T + mT_c + T_c/2$ over one symbol duration plus delay spread, i.e., $m = 0, 1, \ldots, M + L - 2$. Assuming user 1 to be the desired user, the resulting chip-sampled data over the ith symbol can be put into the $(M + L - 1) \times 1$ vector:

$$\begin{aligned} \mathbf{x}(i) &= [x(0), x(1), \cdots, x(M + L - 2)]^T \\ &= \sum_{k=1}^{K} \sqrt{P_k} \sum_{l=1}^{L} \alpha_{k,l} \mathbf{c}_{k,l} d_k(i) + \mathbf{n}(i) \\ &= \mathbf{h}_1 d_1(i) + \textstyle\sum_{k=2}^{K} \mathbf{h}_k d_k(i) + \mathbf{n}(i) \\ &= \mathbf{s}_1(i) + \mathbf{i}(i) + \mathbf{n}(i) , \end{aligned} \tag{5}$$

where T denotes the transpose, $\mathbf{c}_{k,l}$ is the augmented signature vector associated with the lth path of user k, given by the lth column of the $(M+L-1)\times L$ matrix:

$$\mathbf{C}_k = \begin{bmatrix} c_k[0] & 0 & \cdots & 0 \\ \vdots & c_k[0] & \ddots & \vdots \\ c_k[M-1] & \vdots & \ddots & 0 \\ 0 & c_k[M-1] & \ddots & c_k[0] \\ \vdots & \vdots & \ddots & \vdots \\ 0 & 0 & \cdots & c_k[M-1] \end{bmatrix} = \left[\mathbf{c}_{k,1}\mathbf{c}_{k,2}\cdots\mathbf{c}_{k,L}\right] \tag{6}$$

and $\mathbf{h}_k$ is the effective composite signature vector (CSV) of user k given by:

$$\mathbf{h}_k = \sqrt{P_k}\sum_{l=1}^{L}\alpha_{k,l}\mathbf{c}_{k,l}\,. \tag{7}$$

Finally, $\mathbf{s}_1(i) = \mathbf{h}_1 d_1(i)$ is the desired signal vector, $\mathbf{i}(i) = \sum_{k=2}^{K}\mathbf{h}_k d_k(i)$ is the MAI vector involving users 2 to K, and $\mathbf{n}(i)$ is the noise vector.

A receiver for user 1 is designed to identify and remove $\mathbf{h}_1$ to retrieve $d_1(i)$ from $\mathbf{i}(i)$ and $\mathbf{n}(i)$. In particular, a linear receiver combines $\mathbf{x}(i)$ using a weight vector $\mathbf{w}$ to obtain

$$d_1(i) = \mathbf{w}^H\mathbf{x}(i)\,, \tag{8}$$

where H denotes the complex conjugate transpose. For example, the weight vector of the MMSE receiver [12] is chosen in accordance with:

$$\mathbf{w}_{\mathrm{MMSE}} = \mathbf{R}_x^{-1}\mathbf{h}_1\,, \tag{9}$$

where $\mathbf{R}_x$ is the data correlation matrix given by

$$\mathbf{R}_x = E\{\mathbf{x}(i)\mathbf{x}(i)^H\} = \mathbf{R}_s + \mathbf{R}_{in}\,, \tag{10}$$

where

$$\mathbf{R}_s = E\{\mathbf{s}_1(i)\mathbf{s}_1(i)^H\} = \mathbf{h}_1\mathbf{h}_1^H \tag{11}$$

$$\mathbf{R}_{in} = E\{(\mathbf{i}(i)+\mathbf{n}(i))(\mathbf{i}(i)+\mathbf{n}(i))^H\} = \sum_{k=2}^{K}\mathbf{h}_k\mathbf{h}_k^H + \sigma_n^2\mathbf{I} \tag{12}$$

are the signal and interference-plus-noise correlation matrices, respectively. Another type of optimal receiver is the maximum SINR (MSINR) receiver [12] given by

$$\mathbf{w}_{\mathrm{MSINR}} = \mathbf{R}_{in}^{-1}\mathbf{h}_1\,. \tag{13}$$

With the signal component removed before weight computation in (13), improved performance can be achieved especially when the data sample size is small. However, $\mathbf{R}_{in}$ is not available in practice, and usually estimated by decision aided schemes.

As an alternative to the MMSE and MSINR receivers, the MOE detector does not require the explicit channel information [6, 9]. It is designed to minimize the output energy subject to one or more constraints that ensure the gain to the desired user is held constant. The MOE detector is similar to the LCMV beamformer used in adaptive array processing and derives its weight vector according to [9]

$$\min_{\mathbf{w}} \ \mathbf{w}^H \mathbf{R}_x \mathbf{w}$$

$$\text{subject to } \mathbf{D}^H \mathbf{w} = \mathbf{f}, \tag{14}$$

where $\mathbf{D}$ is the $(M + L - 1) \times G$ constraint matrix and $\mathbf{f}$ is a $G \times 1$ response vector specified to control the spectral response. The solution to (14) is given by

$$\mathbf{w}_{\text{MOE}} = \mathbf{R}_x^{-1}\mathbf{D}\left[\mathbf{D}^H\mathbf{R}_x^{-1}\mathbf{D}\right]^{-1}\mathbf{f}. \tag{15}$$

It is shown that the MOE detector approaches the MMSE detector under good channel conditions (i.e., little or no multipath fading) [6]. With no multipaths present, it is natural to choose $\mathbf{D} = \mathbf{c}_{1,1}$ and $\mathbf{f} = 1$ such that $\mathbf{w}_{\text{MOE}} \propto \mathbf{R}_x^{-1}\mathbf{c}_{1,1}$. However, such solution exhibits poor performance over multipath channels due to the signal cancellation phenomenon. A suitable choice for $\mathbf{D}$ and $\mathbf{f}$ can alleviate this undesired effect [8, 9]. The MOE receivers are considered "blind" because they do not need pilot symbols for channel estimation.

3. Development of Partially Adaptive CDMA Multi-User Receiver

In this section, a pre-despread CDMA multi-user receiver is developed which offers the performance of the MMSE or MSINR receiver. The receiver consists of a set of adaptive correlators and a RAKE combiner. A decision aided scheme is included for performance enhancement. In particular, partial adaptivity is incorporated for reduced complexity implementation, and a decorrelating procedure is proposed to avoid the matrix inversion required in computing the adaptive weights. The schematic diagram of the receiver is depicted in Figure 1. The notations in the figure will be defined and made clear in the subsequent development.

3.1. Construction of Blind Adaptive GSC Correlators

A set of adaptive correlators is used to perform despreading and MAI suppression. They are realized in the form of GSC, and require no pilot symbols for channel estimation. In other words, these correlators are "blind" and can utilize the entire received symbols, including data and pilot, to compute the adaptive weights. This is in contrast to non-blind pilot aided methods (e.g., MMSE) which cannot achieve reliable channel estimation in the presence of strong MAI by using the limited number of pilot symbols.

In order to restore the processing gain and retain the path diversity, $\mathbf{x}(i)$ is despread at each of the L fingers using a set of discrete-time correlators:

$$z_{1,l}(i) = \mathbf{w}_l^H\mathbf{x}(i) = \mathbf{w}_l^H\mathbf{h}_1 d_1(i) + \mathbf{w}_l^H\mathbf{i}(i) + \mathbf{w}_l^H\mathbf{n}(i) \tag{16}$$

for $l = 1, \ldots, L$, where $\mathbf{w}_l$ is the correlator weight vector at the lth finger. For an effective suppression of MAI, these weight vectors can be determined in accordance with the LCMV criterion:

$$\min_{\mathbf{w}_l} \ \mathbf{w}_l^H \mathbf{R}_x \mathbf{w}_l$$

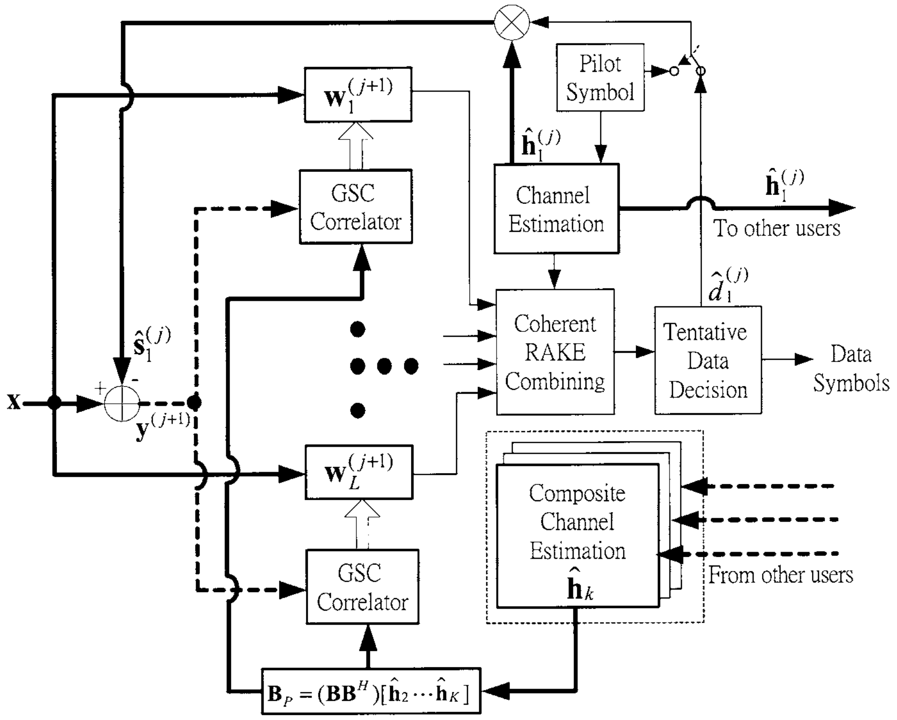

Figure 1. Structure of proposed decision aided CDMA receiver with partially adaptive decorrelating multi-user detection.

$$\text{subject to } \mathbf{c}_{1,l}^H \mathbf{w}_l = 1\,. \tag{17}$$

However, the adverse phenomenon of signal cancellation usually occurs with the solution in (17) due to the mismatch of signature vectors (i.e., mismatch between $\mathbf{c}_{1,l}$ and $\mathbf{h}_1$). With such a mismatch present, the signal can be treated as interference and receive a very small gain. To avoid such signal cancellation, the LCMV correlators can be implemented with multiple constraints [9]. Here an alternative solution is suggested based on the GSC technique. The GSC is essentially an indirect but simpler implementation of the LCMV receiver. It is a widely used structure that allows a constrained adaptive algorithm to be implemented in an unconstrained fashion [7]. The concept of GSC, as depicted in Figure 2(a), is to decompose the weight vector into two orthogonal components as $\mathbf{w}_l = \mathbf{c}_{1,l} - \mathbf{B}\mathbf{u}_l$. The matrix $\mathbf{B}$ is a pre-designed signal "blocking matrix" which removes user 1's signal before filtering. The goal is then to choose the adaptive weight vector $\mathbf{u}_l$ to cancel the interference in $\mathbf{x}(i)$. According to the GSC scheme, $\mathbf{u}_l$ is determined via the MMSE criterion:

$$\min_{\mathbf{u}_l} E\{|\mathbf{c}_{1,l}^H \mathbf{x}(i) - \mathbf{u}_l^H \mathbf{B}^H \mathbf{x}(i)|^2\} \equiv \|\mathbf{R}_x^{1/2}\mathbf{B}\mathbf{u}_l - \mathbf{R}_x^{1/2}\mathbf{c}_{1,l}\|^2\,. \tag{18}$$

Since the signal has been removed in the lower branch by $\mathbf{B}$, the only way to minimize the MSE is such that $\mathbf{u}_l$ performs a mutual cancellation of the MAI between the upper and lower branches. Solving for $\mathbf{u}_l$ and substituting in $\mathbf{w}_l = \mathbf{c}_{1,l} - \mathbf{B}\mathbf{u}_l$, we get

$$\mathbf{w}_l = \left[\mathbf{I} - \mathbf{B}(\mathbf{B}^H \mathbf{R}_x \mathbf{B})^{-1}\mathbf{B}^H \mathbf{R}_x\right]\mathbf{c}_{1,l}\,. \tag{19}$$

This is called the direct-matrix-inversion (DMI) implementation of the fully adaptive (FA) GSC correlators.

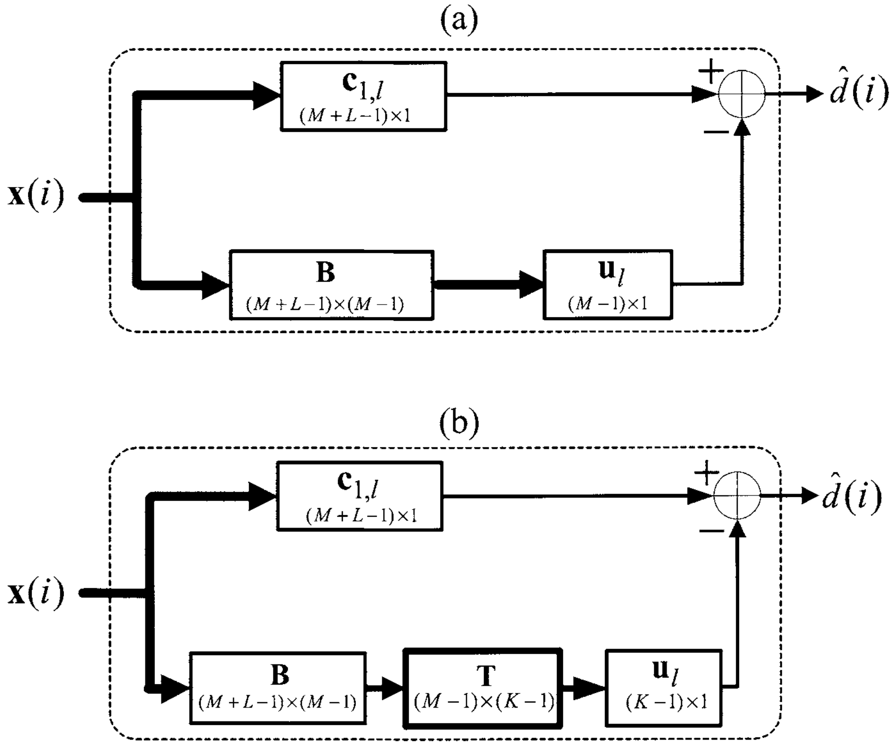

Figure 2. Illustration of (a) fully adaptive GSC, (b) partially adaptive GSC.

Note that $\mathbf{B}$ must block signals from the entire delay spread in order to avoid signal cancellation. It can be chosen to be a full rank $(M+L-1) \times (M-1)$ matrix whose columns are orthogonal to $\{\mathbf{c}_{1,1}, \ldots, \mathbf{c}_{1,L}\}$, i.e., $\mathbf{B}^H\mathbf{C}_1 = \mathbf{O}$. In the DMI implementation, the computation of adaptive weight vectors in (19) involves the inversion of $\mathbf{B}^H\mathbf{R}_x\mathbf{B}$, which is $M \times M$. With a large M, this requires a high computational load and is likely to incur numerical instability and poor convergence behaviors [7]. To alleviate this problem, the partially adaptive (PA) GSC is proposed which uses only a portion of the available degrees of freedom offered by the adaptive weights. Specifically, the PA techniques can be employed to reduce the size of $\mathbf{B}$ or dimension of $\mathbf{u}_l$s [10, 11]. Here a technique suitable for multi-user scenarios is developed.

3.2. Partially Adaptive GSC for Multi-user Scenarios

The PA GSC, as shown in Figure 2(b), works with $K-1$ $(K < M)$ adaptive weights through the use of an $(M-1) \times (K-1)$ linear transformation $\mathbf{T}$ [7, 13]. The criteria for the selection of $\mathbf{T}$ include: (i) K should be as small as possible (ii) MAI should be retained as much as possible in the lower branch. Criterion (i) is for complexity reduction and (ii) is for optimal mutual cancellation of MAI in the upper and lower branches [14]. Criterion (ii) can be further elaborated by noting from (18) that the optimal $\mathbf{u}_l$ leads to a vector lying in the subspace $R\{\mathbf{R}_x^{1/2}\mathbf{B}\}$ that is closest to $\mathbf{R}_x^{1/2}\mathbf{c}_{1,l}$, where $R\{\cdot\}$ denotes the range or column space of a matrix. In other words, $\mathbf{R}_x^{1/2}\mathbf{B}\mathbf{u}_l$ should be in the direction that exhibits maximum "correlation" with $\mathbf{R}_x^{1/2}\mathbf{c}_{1,l}$. It is therefore desired that the blocking matrix $\mathbf{B}$ be chosen such that the crosscorrelation $\rho = |\mathbf{c}_{1,l}^H\mathbf{R}_x\mathbf{B}\mathbf{u}_l|$ is large. In other words, the essential criterion for choosing a reduced size blocking matrix for implementing partial adaptivity is such that the upper and lower branch outputs of the GSC have a large crosscorrelation [14]. Since the lower branch contains no signal, the only way to maximize the crosscorrelation is to retain as much MAI as possible in the lower branch. This in turn suggests that a suitable method for implementing the PA receiver is to find a reduced size **B** that can retain as much MAI as possible. By doing so, a maximum mutual cancellation of interference can be achieved between the upper and lower branches.

Based on criterion (ii), a simple PA scheme is suggested for a multi-user scenario in which user 1 is detected in the presence of $K-1$ dominant MAIs (users 2 to K) whose CSV estimates are readily available to the system by previously done pilot aided channel estimation. Specifically, from (7), the estimated $(M+L-1)\times 1$ CSV of user k can be expressed as

$$\hat{\mathbf{h}}_k = \sum_{l=1}^{L} \hat{\alpha}_{k,l}\mathbf{c}_{k,l} \tag{20}$$

for $k=2,\ldots,K$, where $\hat{\alpha}_{k,l}$ is the channel gain estimate at the lth finger. Given these CSV estimates, a reduced size blocking matrix $\mathbf{B}_P$ retaining the maximum MAI can be constructed by projecting onto the column space of **B** the set of vectors $\{\hat{\mathbf{h}}_k\}$:

$$\mathbf{B}_P = \mathbf{B}\mathbf{B}^H\left[\hat{\mathbf{h}}_2,\ldots,\hat{\mathbf{h}}_K\right], \tag{21}$$

where we assume orthonormal columns of **B** such that $\mathbf{B}^H\mathbf{B}=\mathbf{I}$. Comparing with Figure 2(b), the linear transformation **T** following **B** is $\mathbf{T}=\mathbf{B}^H\left[\hat{\mathbf{h}}_2,\ldots,\hat{\mathbf{h}}_K\right]$. Simple algebra shows that $\mathbf{B}_P$ is an $(M+L-1)\times(K-1)$ matrix which removes the signal and retains as much MAI as possible in the sense of maximum crosscorrelation. PA realization via (21) is simple and proves robust to errors in MAI's channel estimates. In particular, errors in $\hat{\mathbf{h}}_k$s tend to decrease the crosscorrelation between the upper and lower branches, and results in only slight performance degradation. The robustness of the proposed receiver will be shown analytically in Section 4.2. When viewed as a multi-user detector, the proposed PA receiver is much more robust than the conventional ones, which detect and subtract the MAI [1]. In conventional multi-user interference cancellers, a small error in the MAI's channel estimate can result in an enhanced MAI power and possible error propagation.

Note that $\mathbf{B}_P$ can be regarded as the "smallest" blocking matrix with the number of columns (degree of freedom for MAI suppression) equal to the number of detected MAI. If the PA receiver performs $(K-1)$-dim processing, where $K\le M$, then at most $K-1$ MAIs can be suppressed. By doing so, the GSC can concentrate on those dominant MAIs with the smallest possible degree of freedom, leading to lower complexity and better convergence. Finally, substituting (21) in (18) and (19) gives the PA weight vectors:

$$\mathbf{w}_l = \left[\mathbf{I}-\mathbf{B}_P(\mathbf{B}_P^H\mathbf{R}_x\mathbf{B}_P)^{-1}\mathbf{B}_P^H\mathbf{R}_x\right]\mathbf{c}_{1,l} \tag{22}$$

which involves the inversion of the $(K-1)\times(K-1)$ matrix $\mathbf{B}_P^H\mathbf{R}_x\mathbf{B}_P$.

3.3. A New GSC Structure Based on MAI Decorrelation

The incorporation of partial adaptivity according to (21) leads to the development of a new structure of GSC in which no matrix inversion is required. This involves the following procedure. First, the Gram-Schmidt orthogonalization is applied in the subspace $R\{\mathbf{B}\}$ to construct the matrix $\tilde{\mathbf{B}}_P=\left[\tilde{\mathbf{b}}_2,\ldots,\tilde{\mathbf{b}}_K\right]$ whose columns form an orthonormal basis for $R\{\mathbf{B}_P\}$ [15]:

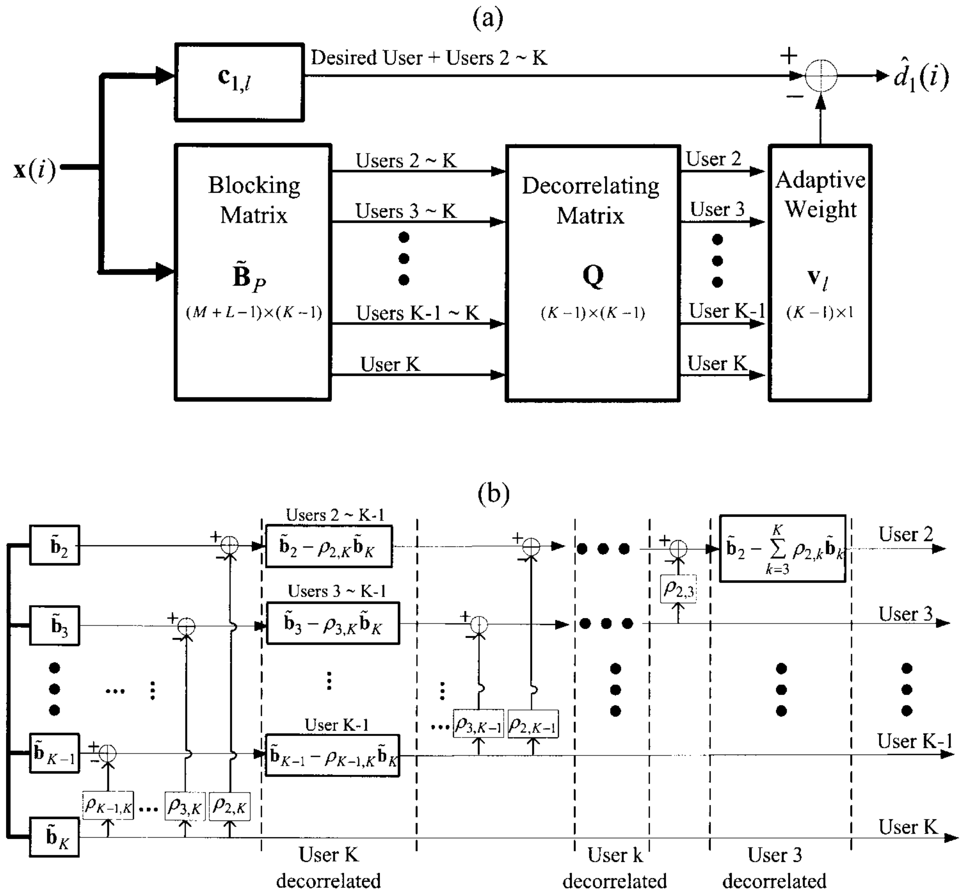

Figure 3. New GSC structure based on MAI decorrelation. (a) Schematic diagram. (b) MAI decorrelation.

1. Initialization: $\mathbf{P}_1^{\perp} = \mathbf{B}\mathbf{B}^H$
2. For $k = 2, \ldots, K$:

$$\tilde{\mathbf{b}}_k = \mathbf{P}_{k-1}^{\perp}\hat{\mathbf{h}}_k$$

$$\mathbf{P}_k^{\perp} = \mathbf{P}_{k-1}^{\perp} - \frac{\tilde{\mathbf{b}}_k\tilde{\mathbf{b}}_k^H}{\tilde{\mathbf{b}}_k^H\tilde{\mathbf{b}}_k}$$

$$\tilde{\mathbf{b}}_k = \tilde{\mathbf{b}}_k/\|\tilde{\mathbf{b}}_k\|$$

An interesting observation gleaned from the above procedure is that $\tilde{\mathbf{b}}_k^H\hat{\mathbf{h}}_j = 0$ for $j < k$ (see Appendix). This means that if $\tilde{\mathbf{B}}_P$ is used in place of $\mathbf{B}_P$ as the blocking matrix, and $\hat{\mathbf{h}}_k$s are accurate enough, then the kth output of $\tilde{\mathbf{B}}_P$ (i.e., $\tilde{\mathbf{b}}_k^H\mathbf{x}(i)$) contains essentially only signals of users k to K, as illustrated in Figure 3(a). This property leads naturally to the following "decorrelated" version of GSC.

Consider the block diagram in Figure 3(b), in which the Kth outputs of $\tilde{\mathbf{B}}_P$ are subtracted from the $(K-1)$th output via the "scalar" GSC criterion:

$$\min_{\rho_{K-1,K}} E\{|\tilde{\mathbf{b}}_{K-1}^H\mathbf{x}(i) - \rho_{K-1,K}^*\tilde{\mathbf{b}}_K^H\mathbf{x}(i)|^2\}, \tag{23}$$

where $\rho_{K-1,K}$ is the adaptive weight. It is noteworthy that after the subtraction, the new $(K-1)$th output contains nearly the $(K-1)$th user signal only. The solutions to (23) is easily derived as

$$\rho_{K-1,K} = \frac{\tilde{\mathbf{b}}_K^H \mathbf{R}_x \tilde{\mathbf{b}}_{K-1}}{\tilde{\mathbf{b}}_K^H \mathbf{R}_x \tilde{\mathbf{b}}_K}\,. \tag{24}$$

Similarly, the Kth and new $(K-1)$th outputs are subtracted from the $(K-2)$th output via

$$\min_{\rho_{K-2,K}} E\{|\tilde{\mathbf{b}}_{K-2}^H \mathbf{x}(i) - \rho_{K-2,K}^* \tilde{\mathbf{b}}_K^H \mathbf{x}(i)|^2\}$$

$$\min_{\rho_{K-2,K-1}} E\{|(\tilde{\mathbf{b}}_{K-2} - \rho_{K-2,K}\tilde{\mathbf{b}}_K)^H \mathbf{x}(i) - \rho_{K-2,K-1}^*(\tilde{\mathbf{b}}_{K-1} - \rho_{K-1,K}\tilde{\mathbf{b}}_K)^H \mathbf{x}(i)|^2\}\,. \tag{25}$$

After the subtraction, the new $(K-2)$th output contains nearly the $(K-2)$th user signal only. The solutions to these adaptive weights are

$$\rho_{K-2,K} = \frac{\tilde{\mathbf{b}}_K^H \mathbf{R}_x \tilde{\mathbf{b}}_{K-2}}{\tilde{\mathbf{b}}_K^H \mathbf{R}_x \tilde{\mathbf{b}}_K}$$

$$\rho_{K-2,K-1} = \frac{(\tilde{\mathbf{b}}_{K-1} - \rho_{K-1,K}\tilde{\mathbf{b}}_K)^H \mathbf{R}_x (\tilde{\mathbf{b}}_{K-2} - \rho_{K-2,K}\tilde{\mathbf{b}}_K)}{(\tilde{\mathbf{b}}_{K-1} - \rho_{K-1,K}\tilde{\mathbf{b}}_K)^H \mathbf{R}_x (\tilde{\mathbf{b}}_{K-1} - \rho_{K-1,K}\tilde{\mathbf{b}}_K)}\,. \tag{26}$$

Proceeding with the same algorithm, we get the expressions for all $\rho_{j,k}$s, $k = 2, \ldots, K$, $j = 2, \ldots, k-1$:

$$\rho_{j,k} = \frac{(\tilde{\mathbf{b}}_k - \sum_{n=k+1}^K \rho_{k,n}\tilde{\mathbf{b}}_n)^H \mathbf{R}_x (\tilde{\mathbf{b}}_j - \sum_{m=k+1}^K \rho_{j,m}\tilde{\mathbf{b}}_m)}{(\tilde{\mathbf{b}}_k - \sum_{n=k+1}^K \rho_{k,n}\tilde{\mathbf{b}}_n)^H \mathbf{R}_x (\tilde{\mathbf{b}}_k - \sum_{n=k+1}^K \rho_{k,n}\tilde{\mathbf{b}}_n)} \tag{27}$$

which is the adaptive weight used for subtracting the kth output from the jth output, as shown in Figure 3(b). The above procedure can be shown to be equivalent to the following transformation on the input data:

$$\tilde{\mathbf{x}}(i) = (\tilde{\mathbf{B}}_P \mathbf{Q})^H \mathbf{x}(i)\,, \tag{28}$$

where $\mathbf{Q}$ is lower triangular matrix having the following form:

$$\mathbf{Q} = \begin{bmatrix} 1 & 0 & 0 & \cdots & 0 \\ -\rho_{2,3} & 1 & 0 & \cdots & 0 \\ \rho_{2,3}\rho_{3,4} - \rho_{2,4} & -\rho_{3,4} & \ddots & \cdots & 0 \\ \vdots & \vdots & \vdots & 1 & \vdots \\ -\sum_{n=3}^K \rho_{2,n} q_{n-1,K-1} & -\sum_{n=4}^K \rho_{3,n} q_{n-1,K-1} & \cdots & -\rho_{K-1,K} & 1 \end{bmatrix},$$

where $q_{s,t}$ satisfies the recursion:

$$q_{t,t} = 1$$

$$q_{s,t} = -\sum_{n=s+1}^{t} \rho_{s+1,n+1} q_{n,t} \qquad \text{for } t > s\,. \tag{29}$$

The derivation is straightforward and omitted for brevity.

The matrix $\tilde{\mathbf{B}}_P\mathbf{Q}$ can be regarded as the equivalent blocking matrix, and $\tilde{\mathbf{x}}(i)$ is the data vector whose kth entry contains essentially the kth user signal only. The fact that the MAI signals are "decorrelated" facilitates a simple realization of the GSC in which the $K-1$ adaptive weights are determined individually via the MMSE criterion:

$$\min_{v_{l,k}} E\{|\mathbf{c}_{1,l}^H\mathbf{x}(i) - v_{l,k}^*\mathbf{q}_k^H\tilde{\mathbf{B}}_P^H\mathbf{x}(i)|^2\} \tag{30}$$

for $l = 1, \ldots, L$, $k = 1, \ldots, K-1$, where $\mathbf{q}_k$ is the kth column of $\mathbf{Q}$. The solution is

$$v_{l,k} = \frac{\mathbf{q}_k^H\tilde{\mathbf{B}}_P^H\mathbf{R}_x\mathbf{c}_{1,l}}{\mathbf{q}_k^H\tilde{\mathbf{B}}_P^H\mathbf{R}_x\tilde{\mathbf{B}}_P\mathbf{q}_k}. \tag{31}$$

Note that by doing so we have converted the original problem into a decoupled one in which the $K-1$ MAIs are suppressed independently. The overall weight vectors of the proposed GSC receiver can be expressed as

$$\mathbf{w}_l = \mathbf{c}_{1,l} - \tilde{\mathbf{B}}_P\mathbf{Q}\mathbf{v}_l = \left[\mathbf{I} - \tilde{\mathbf{B}}_P\mathbf{Q}\mathbf{D}\mathbf{Q}^H\tilde{\mathbf{B}}_P^H\mathbf{R}_x\right]\mathbf{c}_{1,l} \tag{32}$$

for $l = 1, \ldots, L$, where

$$\mathbf{v}_l = \left[v_{l,1}, v_{l,2}, \ldots, v_{l,K-1}\right]^T = \mathbf{D}\mathbf{Q}^H\tilde{\mathbf{B}}_P^H\mathbf{R}_x\mathbf{c}_{1,l} \tag{33}$$

with

$$\mathbf{D} = \begin{bmatrix} \frac{1}{\mathbf{q}_1^H\tilde{\mathbf{B}}_P^H\mathbf{R}_x\tilde{\mathbf{B}}_P\mathbf{q}_1} & 0 & \cdots & 0 \\ 0 & \frac{1}{\mathbf{q}_2^H\tilde{\mathbf{B}}_P^H\mathbf{R}_x\tilde{\mathbf{B}}_P\mathbf{q}_2} & \cdots & 0 \\ \vdots & \vdots & \ddots & \vdots \\ 0 & 0 & \cdots & \frac{1}{\mathbf{q}_{K-1}^H\tilde{\mathbf{B}}_P^H\mathbf{R}_x\tilde{\mathbf{B}}_P\mathbf{q}_{K-1}} \end{bmatrix}. \tag{34}$$

Clearly, the equivalent lower branch adaptive weight vector is given by

$$\mathbf{u}_l = \mathbf{Q}\mathbf{v}_l = \mathbf{Q}\mathbf{D}\mathbf{Q}^H\tilde{\mathbf{B}}_P^H\mathbf{R}_x\mathbf{c}_{1,l} \tag{35}$$

which involves no matrix inversion. The above development leads to the decorrelating implementation of the GSC correlators.

The advantage of the decorrelating GSC is twofold: (i) The computation of scalar adaptive weights $\rho_{j,k}$s is highly modularized in that the solutions in (27) have the same form of quadratic ratio. This leads to a great simplification in implementation. (ii) The $K-1$ outputs from $\mathbf{Q}$ can be used to obtain tentative data symbol estimates for users 2 to K. This suggests the development of a decision aided scheme with which these symbol estimates are used to refine the lower branch processing of the GSC. A final remark about the proposed PA receiver is that it does not require very accurate CSV estimates of the MAI to start with. Simulation results show that the degradation in performance is negligible even with a significantly large error in $\hat{\mathbf{h}}_k$s (e.g., 20–25% relative error). This is a distinctive feature not shared by conventional multi-user receivers. As described previously in Section 3.2, the errors in $\hat{\mathbf{h}}_k$s will decrease the crosscorrelation between the two branches of the GSC, and result in slight degradation in output SINR. This will be shown analytically in Section 4.2. To gain further improvement, inaccurate $\hat{\mathbf{h}}_k$s can be refined by using tentative data decisions from the output of $\mathbf{Q}$, as will be described in the next section.

3.4. Refinement of MAI Channel Estimates

As a result of MAI decorrelation, the weight vectors $\tilde{\mathbf{B}}_P\mathbf{q}_{k-1}$, $k = 2, \ldots, K$, can be used to detect symbols of users 2 to K individually. Denote as

$$\hat{z}_k(i) = \mathbf{q}_k^H \tilde{\mathbf{B}}_P^H \mathbf{x}(i) \tag{36}$$

and let

$$\hat{d}_k(i) = dec\{\hat{z}_k(i)\} \tag{37}$$

be the tentative data symbol decisions for user k, where $dec\{\cdot\}$ denotes the symbol decision operator. A simple and natural way to obtain a refined version of $\hat{\mathbf{h}}_k$ would be to use $\hat{d}_k(i)$ as pilot symbols to perform the re-training:

$$\hat{\mathbf{h}}_k' = \frac{1}{N_s} \sum_{i=1}^{N_s} \mathbf{x}(i)\hat{d}_k(i)^*, \tag{38}$$

where N_s is the number of symbols detected. These refined CSVs are then sent back to construct a new PA blocking matrix as

$$\mathbf{B}_P' = \mathbf{B}\mathbf{B}^H \left[\hat{\mathbf{h}}_2', \ldots, \hat{\mathbf{h}}_K'\right] \tag{39}$$

and the decorrelating procedure is executed accordingly as described in the previous section. Simulation results have confirmed that a single refinement can in fact successfully recover the performance loss with the relative error of $\hat{\mathbf{h}}_k$s as large as 100%.

3.5. RAKE Combining and Decision Aided Signal Subtraction

With the adaptive correlator bank constructed, the next step is to perform a maximum ratio combining of the correlator outputs to collect the multipath energy. Since the MAI has been removed, channel estimation (i.e., $\hat{\alpha}_{1,l}$s) for the desired user can be done accurately, leading to improved performance as compared to the conventional RAKE receiver. However, the GSC correlators are a variation of the LCMV receiver and share the same drawback of the latter, e.g., poor convergence. By poor convergence is meant that there is usually a certain performance degradation due to finite data samples. In [16], an analysis of the LCMV beamformer reveals that the main cause of its poor convergence is the presence of a non-zero crosscorrelation in $\mathbf{R}_x$ between the signal and interference-plus-noise due to finite data samples. The crosscorrelation term induces a perturbation on the beamformer weight vector, which in turn causes a drop in output SINR. With the increase of data sample size, this crosscorrelation term gradually vanishes and the LCMV beamformer approaches the MSINR beamformer. The same statements apply to GSC correlators. A natural way to remedy this is then to remove the perturbation term by artificially removing the signal component in $\mathbf{x}(i)$. This suggests an iterative procedure in which the signal is reconstructed with the aid of tentative symbol decisions at the jth iteration, and subtracted from $\mathbf{x}(i)$ at the $(j+1)$th iteration. The design of the decision aided scheme involves the following procedure, and the corresponding schematic diagram is given again in Figure 1.

First, assume that at the jth iteration, the received data $\mathbf{x}(i)$ is despread at the L fingers into:

$$\hat{z}_{1,l}^{(j)}(i) = \mathbf{w}_l^{(j)H}\mathbf{x}(i) \tag{40}$$

for $l = 1, \ldots, L$, where $\mathbf{w}_l^{(j)}$ is obtained by (19), (22) or (32) using the "signal-subtracted" data vector $\mathbf{y}^{(j)}(i)$ as the GSC input:

$$\mathbf{y}^{(j)}(i) = \mathbf{x}(i) - \hat{\mathbf{s}}_1^{(j-1)}(i) \tag{41}$$

with $\hat{\mathbf{s}}_1^{(j-1)}(i)$ being the desired signal estimated at the $(j-1)$th iteration ($\hat{\mathbf{s}}_1^{(0)}(i) = \mathbf{0}$). That is, the correlation matrix $\mathbf{R}_x$ in (19), (22) or (32) is replaced by $\mathbf{R}_y^{(j)} = E\{\mathbf{y}^{(j)}(i)\mathbf{y}^{(j)}(i)^H\}$. With $\hat{z}_{1,l}^{(j)}(i)$ available, the channel gain estimates at the L fingers can be obtained using a sequence of N_p pilot symbols:

$$\hat{\alpha}_{1,l}^{(j)} = \frac{1}{MN_p}\sum_{i=1}^{N_p}\hat{z}_{1,l}^{(j)}(i)d_1(i)^* \tag{42}$$

for $l = 1, \ldots, L$, where M is the normalizing factor accounting for the processing gain. Note that $\hat{\alpha}_{1,l}^{(j)}$ includes the effect of transmit power P_1. Using these channel estimates, a coherent RAKE combining of $\hat{z}_{1,l}^{(j)}(i)$s is achieved by

$$\hat{z}_1^{(j)}(i) = \sum_{l=1}^{L}\hat{\alpha}_{1,l}^{(j)*}\hat{z}_{1,l}^{(j)}(i) \tag{43}$$

which is then sent to the data decision device:

$$\hat{d}_1^{(j)}(i) = dec\{\hat{z}_1^{(j)}(i)\}\,. \tag{44}$$

Second, signal reconstruction is done by exploiting the channel estimates $\hat{\alpha}_{1,l}^{(j)}$s, the desired user's signature $\mathbf{c}_{1,l}$ and symbol decisions $\hat{d}_1^{(j)}(i)$ as follows:

$$\hat{\mathbf{s}}_1^{(j)}(i) = \left(\sum_{l=1}^{L}\hat{\alpha}_{1,l}^{(j)}\mathbf{c}_{1,l}\right)\hat{d}_1^{(j)}(i)\,. \tag{45}$$

Note that $\hat{\alpha}_{1,l}^{(j)}$s are used for both signal reconstruction and symbol detection. Finally, the reconstructed signal is subtracted from the data sent to the $(j+1)$th iteration, which yields

$$\mathbf{y}^{(j+1)}(i) = \mathbf{x}(i) - \hat{\mathbf{s}}_1^{(j)}(i)\,. \tag{46}$$

By using $\mathbf{y}^{(j+1)}(i)$ as the GSC input, the adverse slow convergence can be effectively improved, and the PA CDMA multi-user receiver can achieve its optimal performance with a moderate size of data samples. Due to signal subtraction, the receiver will act like the MSINR receiver operating on $\mathbf{R}_{in}$, which offers the best compromise between MAI plus noise suppression and signal reception. The above described procedure can be iterated $J > 2$ times, if necessary, to gain further improvement.

4. Complexity and Performance Issues

4.1. Computational Complexity

The computational complexity is an issue depending on M and K. For the DMI receivers described in Sections 3.1 and 3.2, the major computation involves the inversion of $[\mathbf{B}^H\mathbf{R}_x\mathbf{B}]^{-1}$ of size $(M-1)\times(M-1)$ in (19), and inversion of $[\mathbf{B}_P^H\mathbf{R}_x\mathbf{B}_P]^{-1}$ of size $(K-1)\times(K-1)$ in (22), respectively. For the decorrelating receiver described in Section 3.3, the PA GSC requires no matrix inversion, but instead the processing of the lower triangular matrix $\mathbf{Q}$. In summary, the approximate complexity (in number of complex multiplications) of the MMSE receiver, FA receiver, DMI PA receiver, and decorrelating PA receiver are given as below:

- MMSE: $O((M+L-1)^3)$
- FA: $O((M-1)\times(M+L-1)^2+(M-1)^3)$
- PA-DMI: $O((K-1)\times(M+L-1)^2+(K-1)^3)$
- PA-Decorrelating: $O((K-1)\times(M+L-1)^2)$

4.2. Performance of Iterative RAKE Receiver

From (22), (32), (40) and (43), the equivalent RAKE receiver weight vector for user 1 is given by

$$\begin{aligned}\mathbf{w} &= \sum_{l=1}^{L}\hat{\alpha}_{1,l}\mathbf{w}_l \\ &= \left[\mathbf{I}-\mathbf{B}_P(\mathbf{B}_P^H\mathbf{R}_{in}\mathbf{B}_P)^{-1}\mathbf{B}_P^H\mathbf{R}_{in}\right]\hat{\mathbf{h}}_1 \quad \text{(DMI receiver)} \\ &= \left[\mathbf{I}-\tilde{\mathbf{B}}_P\mathbf{Q}\mathbf{D}\mathbf{Q}^H\tilde{\mathbf{B}}_P^H\mathbf{R}_{in}\right]\hat{\mathbf{h}}_1 \quad \text{(Decorrelating receiver)},\end{aligned} \tag{47}$$

where we have omitted the superscript (j) and assumed convergence of the iterations such that $\mathbf{R}_y^{(j)}\approx\mathbf{R}_{in}$, and denoted as $\hat{\mathbf{h}}_1=\sum_{l=1}^{L}\hat{\alpha}_{1,l}^{(j)}\mathbf{c}_{1,l}$ the estimated CSV of user 1. The output SINR of the RAKE receiver is given accordingly by

$$\begin{aligned}\text{SINR}_o &= \frac{\mathbf{w}^H\mathbf{R}_s\mathbf{w}}{\mathbf{w}^H\mathbf{R}_{in}\mathbf{w}} \\ &\approx \frac{|\hat{\mathbf{h}}_1^H\mathbf{h}_1|^2}{\hat{\mathbf{h}}_1^H\mathbf{R}_{in}\hat{\mathbf{h}}_1-\hat{\mathbf{h}}_1^H\mathbf{R}_{in}\mathbf{B}_P\left[\mathbf{B}_P^H\mathbf{R}_{in}\mathbf{B}_P\right]^{-1}\mathbf{B}_P^H\mathbf{R}_{in}\hat{\mathbf{h}}_1} \quad \text{(DMI receiver)} \\ &\approx \frac{|\hat{\mathbf{h}}_1^H\mathbf{h}_1|^2}{\hat{\mathbf{h}}_1^H\mathbf{R}_{in}\hat{\mathbf{h}}_1-(\tilde{\mathbf{B}}_P\mathbf{Q}\mathbf{D}\mathbf{Q}^H\tilde{\mathbf{B}}_P^H\mathbf{R}_{in}\hat{\mathbf{h}}_1)^H\mathbf{R}_{in}(\tilde{\mathbf{B}}_P\mathbf{Q}\mathbf{D}\mathbf{Q}^H\tilde{\mathbf{B}}_P^H\mathbf{R}_{in}\hat{\mathbf{h}}_1)} \\ &\qquad \text{(Decorrelating receiver)}.\end{aligned} \tag{48}$$

The denominator of (48) can be rewritten as

$$\begin{aligned}&\hat{\mathbf{h}}_1^H\mathbf{R}_{in}\hat{\mathbf{h}}_1-\hat{\mathbf{h}}_1^H\mathbf{R}_{in}\mathbf{B}_P(\mathbf{B}_P^H\mathbf{R}_{in}\mathbf{B}_P)^{-1}\mathbf{B}_P^H\mathbf{R}_{in}\hat{\mathbf{h}}_1 \\ &\quad = \|\mathbf{R}_{in}^{1/2}\hat{\mathbf{h}}_1\|^2-\|\mathbf{R}_{in}^{1/2}\mathbf{B}_P(\mathbf{B}_P^H\mathbf{R}_{in}\mathbf{B}_P)^{-1}\mathbf{B}_P^H\mathbf{R}_{in}\hat{\mathbf{h}}_1\|^2\end{aligned} \tag{49}$$

It is clear that the goal of designing the PA GSC is to choose a transformation matrix $\mathbf{T}=\mathbf{B}^H\left[\hat{\mathbf{h}}_2,\ldots,\hat{\mathbf{h}}_K\right]$ to minimize (49) such that the maximum SINR_o can be achieved.

It is shown in [18] that the optimal $\mathbf{T}$ is given by $\mathbf{T} = \mathbf{E}_I$, where $\mathbf{E}_I$ consists of the eigenvectors of $\mathbf{B}^H\mathbf{R}_{in}\mathbf{B}$ corresponding to the $K - 1$ largest eigenvalues. Since $R\{\mathbf{E}_I\} = R\{\mathbf{B}^H [\mathbf{h}_2, \ldots, \mathbf{h}_K]\}$, the optimal $\mathbf{T}$ can also be obtained as $\mathbf{T} = \mathbf{B}^H [\mathbf{h}_2, \ldots, \mathbf{h}_K]$, where $\mathbf{h}_k$s are the true CSVs. In practice, $\mathbf{h}_k$s are replaced by their estimates, and the corresponding $\mathbf{B}_P = \mathbf{BT} = \mathbf{BB}^H \left[\hat{\mathbf{h}}_2, \ldots, \hat{\mathbf{h}}_K\right]$ would tend to decrease the squared norm $\|\mathbf{R}_{in}^{1/2}\mathbf{B}_P(\mathbf{B}_P^H\mathbf{R}_{in}\mathbf{B}_P)^{-1}\mathbf{B}_P^H\mathbf{R}_{in}\hat{\mathbf{h}}_1\|^2$, which in turn leads to a certain drop in the SINR_o in (48). Since $\mathbf{R}_{in}^{1/2}\mathbf{B}_P(\mathbf{B}_P^H\mathbf{R}_{in}\mathbf{B}_P)^{-1}\mathbf{B}_P^H\mathbf{R}_{in}\hat{\mathbf{h}}_1$ represents the projection of $\mathbf{R}_{in}^{1/2}\hat{\mathbf{h}}_1$ onto $R\{\mathbf{R}_{in}^{1/2}\mathbf{B}_P\}$, which does not change significantly with $\mathbf{B}_P$, it follows that the degradation in SINR_o would be insignificant as long as the CSV errors are moderately small. This confirms the aforementioned robustness of the receiver to CSV errors.

4.3. Performance of MSINR Receiver

With signal subtraction, the proposed decision aided CDMA receiver will act like the MSINR receiver operating on $\mathbf{R}_{in}$. Thus the same analysis can thus be applied to both. For a manageable derivation, we consider the simple case involving only the signal and a single MAI:

$$\mathbf{x}(i) = \mathbf{h}_1 d_1(i) + \mathbf{h}_2 d_2(i) + \mathbf{n}(i)\,. \tag{50}$$

Assume that the two users have the same channel condition such that $\|\mathbf{h}_k\| = \eta\sqrt{P_k}$, $k = 1, 2$, with $\eta = \|\sum_{l=1}^{L} \alpha_{k,l}\mathbf{c}_{k,l}\|$. In this case, the MSINR weight vector can be rewritten from (13) as (using matrix inversion lemma):

$$\mathbf{w}_{\text{MSINR}} = \frac{1}{\sigma_n^2}\left\{\mathbf{h}_1 - \frac{\sqrt{P_1}\sqrt{P_2}\eta^2\gamma_{12}^*\mathbf{h}_2}{\sigma_n^2 + \eta^2 P_2}\right\}, \tag{51}$$

where $\gamma_{12} = (\mathbf{h}_1^H\mathbf{h}_2)/(\eta^2\sqrt{P_1}\sqrt{P_2})$. The corresponding receiver output SINR can be derived as

$$\text{SINR}_o = \frac{|\mathbf{w}_{\text{MSINR}}^H\mathbf{h}_1|^2}{|\mathbf{w}_{\text{MSINR}}^H\mathbf{h}_2|^2 + \sigma_n^2\mathbf{w}_{\text{MSINR}}^H\mathbf{w}_{\text{MSINR}}} = \frac{\eta^2 P_1[\eta^2 P_2(1 - |\gamma_{12}|^2) + \sigma_n^2]}{\sigma_n^2(\eta^2 P_2 + \sigma_n^2)}\,. \tag{52}$$

Under strong MAI ($P_2 \gg \sigma_n^2$), (52) can be simplified as

$$\text{SINR}_o = \eta^2(1 - |\gamma_{12}|^2)\frac{P_1}{\sigma_n^2} \tag{53}$$

which indicates that the output SINR increases linearly with the input SNR (before combining). An interesting case arises with the assumption that the fading gains $\alpha_{k,l}$s are unit variance i.i.d random variables. In this case, it is easily verified that $E\{\eta^2\} = ML$ and $E\{\gamma_{12}\} = 0$ such that the average output SINR is approximately given by $\text{SINR}_o = MLP_1/\sigma_n^2$, which is the input SNR multiplied by the total gain due to path diversity and despreading.

5. Computer Simulations

Simulation results are demonstrated to confirm the performance of the proposed receiver in a time-multiplexed pilot symbols assisted system. The environment considered is the uplink of a simplified single cell synchronous CDMA system over a slow fading channel. The receiver output SINR is used as the evaluation index. Also, the input SNR is defined as $\mathrm{SNR}_i = P_1/\sigma_n^2$, and the near-far-ratio is defined as $\mathrm{NFR} = P_k/P_1$, $k = 2, \ldots, K$, where we assume equal power MAI for convenience. The channel model adopted for simulations is a Rayleigh multipath fading channel, in which the fading gains, $\alpha_{k,l}$s, are independent, identically distributed complex Gaussian random variables with zero-mean and unit variance. The path delays $\tau_{k,l}$s are assumed uniform over $[0, 3T_c]$, the number of paths is $L = 4$ for all users and the number of fingers of the receiver is $L = 4$. All CDMA signals are generated with BPSK data modulation and Gold codes of length 31 are used as the spreading codes. For each simulation trial, N_s symbols (including data and pilot) are used to obtain the sample estimate of $\mathbf{R}_x$ and $\mathbf{R}_y^{(j)}$ as

$$\hat{\mathbf{R}}_x = \frac{1}{N_s} \sum_{i=1}^{N_s} \mathbf{x}(i)\mathbf{x}(i)^H$$

$$\hat{\mathbf{R}}_y^{(j)} = \frac{1}{N_s} \sum_{i=1}^{N_s} \mathbf{y}^{(j)}(i)\mathbf{y}^{(j)^H}(i)$$

and N_p pilot symbols are used to obtain the $\hat{\alpha}_{1,l}^{(j)}$s in (42). Unless otherwise mentioned, the following parameters are assumed: $K = 10$, $\mathrm{SNR}_i = 0$ dB, $\mathrm{NFR} = 10$ dB, $N_s = 500$, $N_p = 50$, and the number of iterations is $J = 3$. Each simulation result is obtained by the average from 100 independent trials, with each trial using a different set of $\alpha_{k,l}$s and data/noise sequence. For comparison, we also include the results obtained with the ideal MSINR, MMSE and MOE receivers, and analysis results obtained in Sections 4.2 and 4.3. The ideal MSINR receiver is obtained by (13), with the true $\mathbf{R}_{in}$ and $\mathbf{h}_1$ used. The MMSE receiver is obtained by (9), with $\mathbf{R}_x$ replaced by $\hat{\mathbf{R}}_x$ and $\mathbf{h}_1$ estimated using N_p pilot symbols by

$$\hat{\mathbf{h}}_1 = \frac{1}{N_p} \sum_{i=1}^{N_p} \mathbf{x}(i) d_1(i)^* .$$

The MOE receiver is based on the method presented in [8]. Two analysis results are calculated according to the third equation on the right hand side of (48) (denoted as "Proposed PA (Anal.)"), and the maximum average output SINR attainable by the single-user receiver: $\mathrm{SINR}_o = \mathrm{SNR}_i + 10\log_{10} ML$ (denoted as "Optimal"), respectively.

In the first simulation, the output SINR performance of the proposed receiver is evaluated as a function of iteration number J. Included are the FA receiver (in Section 3.1), PA DMI (in Section 3.2) and PA decorrelating (in Section 3.3) receivers. For channel estimation, $N_p = N_s/10$ pilot symbols are used. For the PA receivers, true channel vectors were assumed for the MAI, i.e., $\hat{\mathbf{h}}_k = \mathbf{h}_k$, $k = 2, \ldots, K$. The results in Figure 4 show that the proposed three receivers successively approach the ideal MSINR receiver in three iterations. After convergence, the two PA receivers have almost the same performance of the FA receiver, confirming that the reduced dimension transformation in (21) retains the full interference suppression capability of the FA receiver.

In the second simulation, the robustness of the proposed PA receivers against MAI channel estimation errors is demonstrated. In this case, $\hat{\mathbf{h}}_k = \mathbf{h}_k + \sigma_h \Delta\mathbf{h}$, where $\Delta\mathbf{h}$ is a random vector with the entries being i.i.d. complex Gaussian random variables with the same variance of 4. Note that the entries of $\mathbf{h}_k$ are i.i.d. complex Gaussian random variables with variance

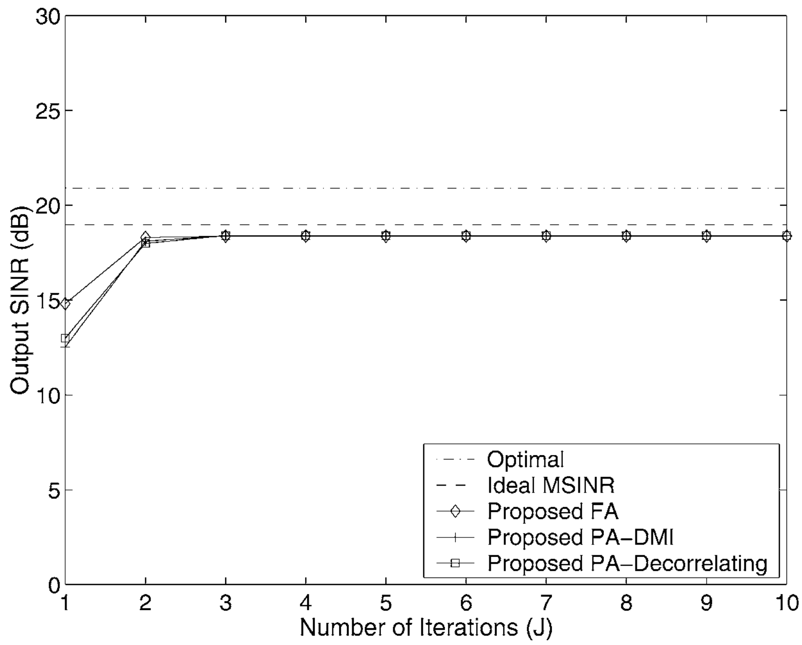

Figure 4. Output SINR versus number of iterations J, with $K = 10$, $\text{SNR}_i = 0$ dB, NFR $= 10$ dB and $N_s = 500$.

$LP_k = 4P_k$. Figure 5 shows the output SINR versus $\sigma_h/\sqrt{P_k}$, which is a measure of the relative channel estimation error. The results confirm that the proposed PA receivers can perform quite reliably for up to a 20–25% relative error in MAI channel estimation. Furthermore, with channel refinement (CR) incorporated as described in (39), the PA receiver can successfully recover the performance loss even with a 100% relative channel error. As a multi-user detector, the proposed PA receivers exhibits a much better robustness than conventional multi-user interference cancellers such as PIC and SIC [4], which are very sensitive to channel errors. In the following simulations, only the PA decorrelating receiver will be examined for the sake of brevity, and true CSVs of MAI are always assumed.

The third simulation compares the convergence behaviors of the proposed receiver with the MMSE and MOE receivers. The proposed receiver uses $N_p = N_s/10$ pilot symbols, and the MMSE receiver uses either $N_p = N_s/10$ or $N_p = N_s$ (full) pilot symbols. The MOE receiver is considered as blind with $N_p = 0$. The results given in Figure 6 show that the proposed receiver with $1/10$ pilot symbols converges in about 200 data symbols and is only 1 dB away from the ideal MSINR receiver. On the other hand, the MMSE receiver using full pilot symbols offers nearly the performance of the ideal MSINR receiver, but degrades significantly if only $1/10$ pilot symbols are available. The reasons for the significant discrepancy between the proposed and MMSE receivers with a low pilot symbol ratio is that the proposed receiver cancels the MAI before channel estimation whereas the MMSE receiver estimates the channel in the presence of strong MAI. The MOE receiver is better than the MMSE receiver with $1/10$ pilot symbols for a small N_s, but is inferior to the proposed receiver by about 9 dB. Although the MOE receiver is known to approach the MMSE receiver under good conditions such as high SNR and moderate multipath fading and MAI, it is unable to maintain the same performance under the severe conditions assumed in the simulation. A close investigation of the simulation results reveals that the MOE receiver successfully cancels the MAI, but gives a

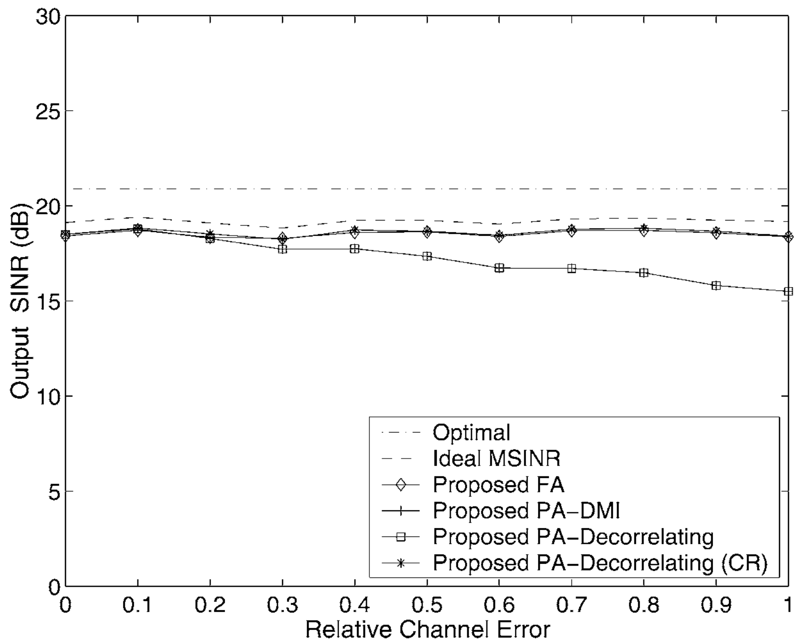

Figure 5. Output SINR versus relative channel estimation error $\sigma_h/\sqrt{P_k}$, with $K = 10$, $\text{SNR}_i = 0$ dB, NFR = 10 dB, $N_s = 500$ and $J = 3$.

low gain for the desired signal due to channel mismatch. Note that pilot symbols can be used for the MOE receiver to obtain the channel phase, but this does not make any difference to its output SINR performance.

In the fourth simulation, the output SINR performance is evaluated as a function of input SNR. The results shown in Figure 7 indicate that the proposed receiver successively approaches the ideal MSINR receiver within a wide range of input SNR, confirming that the MAIs were indeed successfully suppressed by the GSC correlators, and PA implementation can retain the performance of the FA receiver. In the fifth simulation, the system capacity is evaluated with different values of K. As shown in Figure 8, the proposed receiver is able to offer the performance of the ideal MSINR receiver in a heavily loaded system with effective MAI suppression. In the sixth simulation, the near-far resistance is evaluated with different NFR values. Figure 9 shows the output SINR curves. It is observed that both the proposed and MMSE receivers achieve their excellent near-far resistance by successfully cancelling the MAI using the temporal degree of freedom offered by the pre-despread data.

Finally, the bit error rate (BER) performance of the proposed receiver is compared with the decorrelating and multistage multi-user detectors. The results are shown in Figure 10. The decorrelating detector is based on the well known method described in [3], and the multistage detector is implemented with the decorrelating detector as its first stage and PIC as the second stage [3]. The proposed receiver uses $N_p = N_s/10$ pilot symbols, and both multi-user detectors use either $N_p = N_s/10$ or $N_p = N_s$ (full) pilot symbols for channel estimation. The single-user lower bound is also included as a benchmark for evaluation [17]. The results show that the proposed receiver significantly outperforms the two multi-user detectors with $1/10$ pilot symbols, which confirms again the advantage of the former in robustness to channel

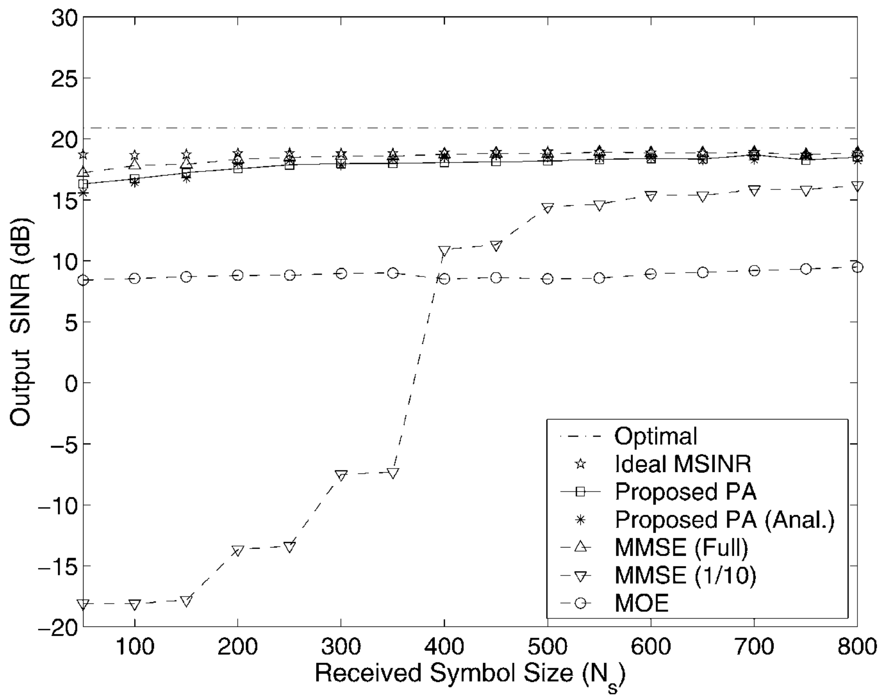

Figure 6. Output SINR versus received symbol size N_s, with $K = 10$, $\text{SNR}_i = 0$ dB, NFR = 10 dB and $J = 3$.

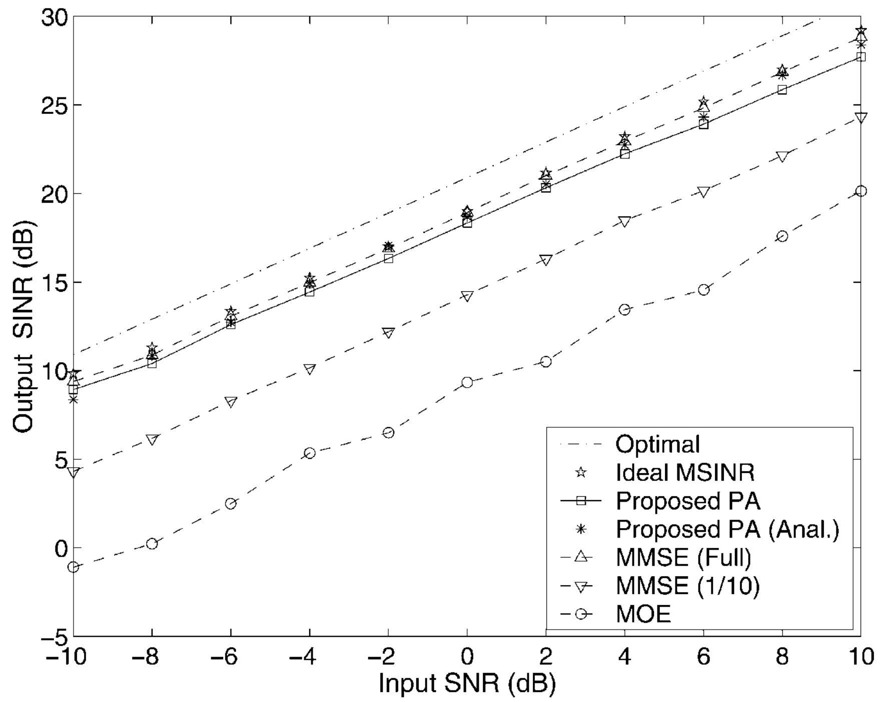

Figure 7. Output SINR versus input SNR, with $K = 10$, NFR = 10 dB, $N_s = 500$ and $J = 3$.

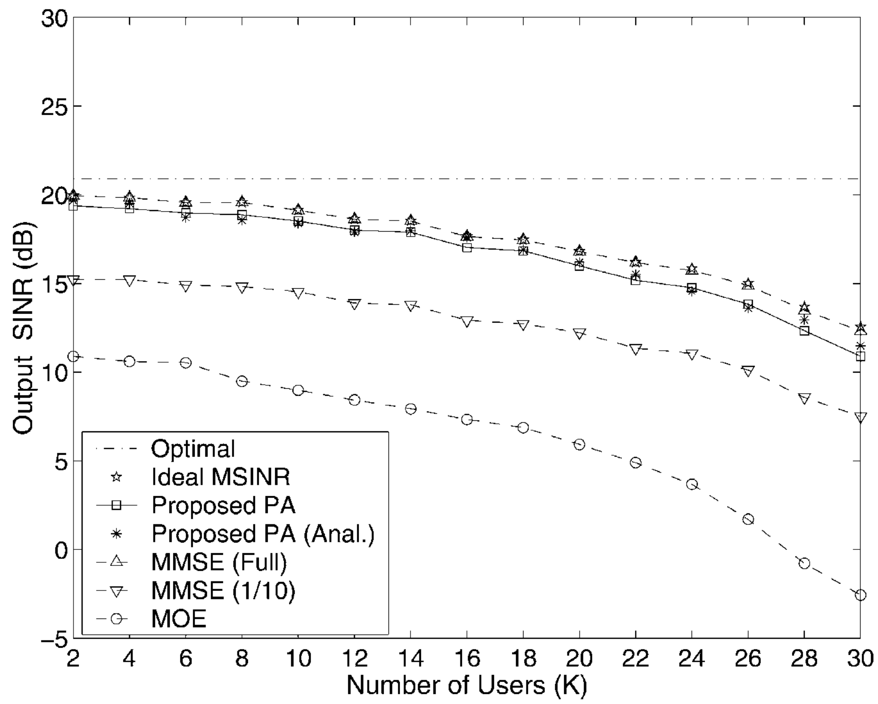

Figure 8. Output SINR versus user number K, with $\mathrm{SNR}_i = 0$ dB, NFR $= 10$ dB, $N_s = 500$ and $J = 3$.

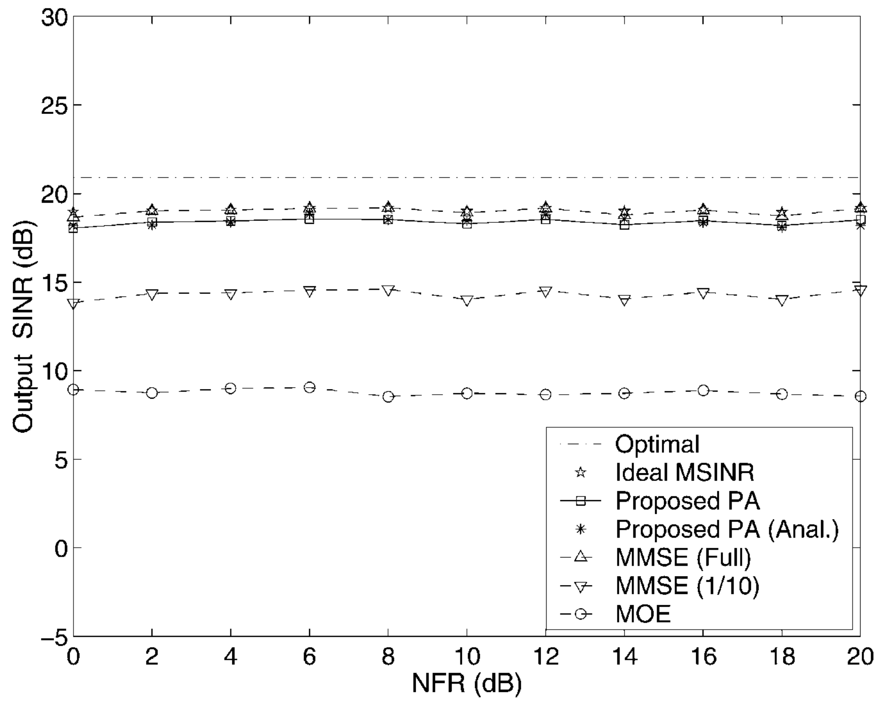

Figure 9. Output SINR versus NFR, with $K = 10$, $\mathrm{SNR}_i = 0$ dB, $N_s = 500$ and $J = 3$.

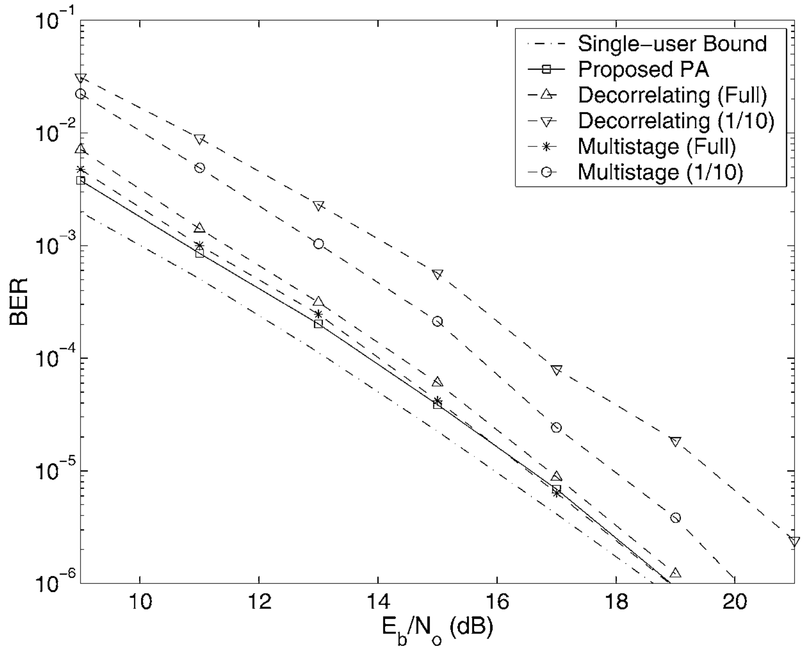

Figure 10. BER versus E_b/N_o, with $K = 10$, NFR = 10 dB, $N_s = 500$ and $J = 3$.

estimation errors. Even with full pilot symbols, these multi-user detectors are still inferior to the proposed receiver by a noticeable margin at low SNR.

6. Conclusion

A decision aided receiver with partially adaptive interference suppression is proposed for CDMA systems over multipath channels. The new receiver is developed with a two-stage procedure. First, blind adaptive correlators are constructed at different fingers based on the GSC scheme to collect multipath signals and suppress strong MAI. For reduced complexity implementation, partial adaptivity is incorporated into the GSC, and this is achieved by projecting onto the column space of the GSC blocking matrix the MAI signature vectors obtained in a multi-user scenario. Furthermore, with a judiciously designed decorrelating procedure, a new GSC structure is obtained in which the MAI are decorrelated and suppressed individually such that matrix inversion involved in computing the GSC weight vectors can be avoided entirely. Second, a simple RAKE combiner with pilot aided channel estimation gives the desired user's symbol decisions. For further performance enhancement, an iterative decision aided scheme is introduced which reconstructs and subtracts the signal from the GSC input data. This effectively eliminates the performance drop due to finite data samples effect. Simulation study shows that the proposed partially adaptive CDMA multi-user receiver is robust to channel estimation errors, outperforms conventional multi-user detectors, and achieves nearly the same performance of the ideal MSINR and MMSE receivers under severe environmental conditions. The main advantages of the proposed receiver over others lie in a lower implementation complexity and overhead for pilot symbols.

References

1. S. Moshavi, "Multi-User Detection for DS-CDMA Communications", *IEEE Communications Magazine*, Vol. 34, pp. 124–136, 1996.
2. R. Lupas and S. Verdu, "Linear Multiuser Detectors for Synchronous Code-Division Multiple-Access Channels", *IEEE Trans. Inform. Theory*, Vol. 35, pp. 123–136, 1989.
3. S. Verdu, *Multiuser Detection*, Cambridge University Press: NY, 1998.
4. G. Woodward and B.S. Vucetic, "Adaptive Detection for DS-CDMA", *Proc. IEEE*, Vol. 86, pp. 1413–1434, 1998.
5. U. Madhow and M. Honig, "MMSE Interference Suppression for Direct-Sequence Spread-Spectrum CDMA", *IEEE Trans. Commun.*, Vol. 42, pp. 3178–3188, 1994.
6. M. Honig, U. Madhow and S. Verdu, "Blind Adaptive Multiuser Detection", *IEEE Trans. Inform. Theory*, Vol. 41, pp. 944–960, 1995.
7. B.D. Van Veen and K.M. Buckley, "Beamforming: A Versatile Approach to Spatial Filtering", *IEEE ASSP Magazine*, Vol. 5, pp. 4–24, 1988.
8. M.K. Tsatsanis and Z. Xu, "Performance Analysis of Minimum Variance CDMA Receivers", *IEEE Trans. Signal Processing*, Vol. 46, pp. 3014–3022, 1998.
9. Z. Tian, K.L. Bell and H.L. Van Trees, "Robust Constrained Linear Receivers for CDMA Wireless Systems", *IEEE Trans. Signal Processing*, Vol. 49, pp. 1510–1522, 2001.
10. E.G. Ström and S.L. Miller, "Properties of the Single-Bit Single-User MMSE Receiver for DS-CDMA Systems", *IEEE Trans. Commun.*, Vol. 47, pp. 416–425, 1999.
11. J.S. Goldstein and I.S. Reed, "Subspace Selection for Partially Adaptive Sensor Array Processing", *IEEE Trans. Aerospace Electronic Syst.*, Vol. 33, pp. 539–544, 1997.
12. X. Bernstein and A.M. Haimovich, "Space-Time Optimum Combining for CDMA Communications", *Wireless Personal Commun.*, Vol. 3, pp. 73–89, 1996.
13. B.D. Van Veen, "Minimum Variance Beamforming", in S. Haykin and A. Steinhardt (ed.), *Adaptive Radar Detection and Estimation*, John Wiley and Sons: NY, 1992.
14. D.A. Pados and S.N. Batalama, "Low-Complexity Blind Detection of DS/CDMA Signals Auxiliary-Vector Receivers", *IEEE Trans. Commun.*, Vol. 45, pp. 1586–1594, 1997.
15. H. Stark and Y. Yang, *Vector Space Projections*, John Wiley and Sons: NY, 1998.
16. M. Wax and Y. Anu, "Performance Analysis of the Minimum Variance Beamformer", *IEEE Trans. Signal Processing*, Vol. 44, pp. 928–937, 1996.
17. J.G. Proakis, *Digital Communications*, 4th edn, McGraw-Hill: NY, 2001.
18. H. Yang and M.A. Ingram, "Design of Partially Adaptive Arrays Using the Singular-Value Decomposition", *IEEE Trans. Antennas and Propag.*, Vol. 45, pp. 843–850, 1997.

Appendix

First, let $k = 3$ and $j = 2$. $\tilde{\mathbf{b}}_3^H \hat{\mathbf{h}}_2$ can be expressed as follows:

$$\begin{aligned}
\tilde{\mathbf{b}}_3^H \hat{\mathbf{h}}_2 &= (\mathbf{P}_2^{\perp} \hat{\mathbf{h}}_3)^H \hat{\mathbf{h}}_2 \\
&= \hat{\mathbf{h}}_3^H \left(\mathbf{P}_1^{\perp} - \frac{\tilde{\mathbf{b}}_2 \tilde{\mathbf{b}}_2^H}{\tilde{\mathbf{b}}_2^H \tilde{\mathbf{b}}_2} \right) \hat{\mathbf{h}}_2 \\
&= \hat{\mathbf{h}}_3^H \mathbf{P}_1^{\perp} \hat{\mathbf{h}}_2 - \hat{\mathbf{h}}_3^H \left(\frac{\tilde{\mathbf{b}}_2 \tilde{\mathbf{b}}_2^H \hat{\mathbf{h}}_2}{\tilde{\mathbf{b}}_2^H \tilde{\mathbf{b}}_2} \right) \\
&= \hat{\mathbf{h}}_3^H \mathbf{P}_1^{\perp} \hat{\mathbf{h}}_2 - \hat{\mathbf{h}}_3^H \mathbf{P}_1^{\perp} \hat{\mathbf{h}}_2 \left(\frac{\hat{\mathbf{h}}_2^H \mathbf{P}_1^{\perp} \hat{\mathbf{h}}_2}{\hat{\mathbf{h}}_2^H \mathbf{P}_1^{\perp} \hat{\mathbf{h}}_2} \right) \\
&= 0,
\end{aligned}$$

where we use $(\mathbf{P}_2^{\perp})^H = \mathbf{P}_2^{\perp}$ and $(\mathbf{P}_1^{\perp})^2 = \mathbf{P}_1^{\perp}$. Next, assume that $\tilde{\mathbf{b}}_{k'}^H \hat{\mathbf{h}}_j = 0$ holds for $j < k'$. Then for $k = k' + 1$ and $j < k' + 1$, we have

$$\begin{aligned}
\tilde{\mathbf{b}}_{k'+1}^H \hat{\mathbf{h}}_j &= (\mathbf{P}_{k'}^{\perp} \hat{\mathbf{h}}_{k'+1})^H \hat{\mathbf{h}}_j \\
&= \hat{\mathbf{h}}_{k'+1}^H \left(\mathbf{P}_{j-1}^{\perp} - \frac{\tilde{\mathbf{b}}_j \tilde{\mathbf{b}}_j^H}{\tilde{\mathbf{b}}_j^H \tilde{\mathbf{b}}_j} - \sum_{n=j+1}^{k'} \frac{\tilde{\mathbf{b}}_n \tilde{\mathbf{b}}_n^H}{\tilde{\mathbf{b}}_n^H \tilde{\mathbf{b}}_n} \right) \hat{\mathbf{h}}_j \\
&= \hat{\mathbf{h}}_{k'+1}^H \mathbf{P}_{j-1}^{\perp} \hat{\mathbf{h}}_j - \hat{\mathbf{h}}_{k'+1}^H \left(\frac{\tilde{\mathbf{b}}_j \tilde{\mathbf{b}}_j^H}{\tilde{\mathbf{b}}_j^H \tilde{\mathbf{b}}_j} \right) \hat{\mathbf{h}}_j \\
&= \hat{\mathbf{h}}_{k'+1}^H \mathbf{P}_{j-1}^{\perp} \hat{\mathbf{h}}_j - \hat{\mathbf{h}}_{k'+1}^H \mathbf{P}_{j-1}^{\perp} \hat{\mathbf{h}}_j \left(\frac{\hat{\mathbf{h}}_j^H \mathbf{P}_{j-1}^{\perp} \hat{\mathbf{h}}_j}{\hat{\mathbf{h}}_j^H \mathbf{P}_{j-1}^{\perp} \hat{\mathbf{h}}_j} \right) \\
&= 0.
\end{aligned}$$

Gau-Joe Lin was born in Chyayi, Taiwan, R.O.C., in 1963. He received the B.S.E.E. degree from Chung Cheng Institute of Technology, Taoyuan, Taiwan, in 1986, and the M.S.E.E. degree from National Sun Yat-Sen University, Kaohsiung, Taiwan, in 1991. Currently he is working toward the Ph.D. degree in the Department of Communication Engineering at National Chiao Tung University, Hsinchu, Taiwan. From 1986 to 1989 and 1991 to 1999, he was in the C3I department at Chung Shan Institute of Science and Technology, Taoyuan, Taiwan. His research interests include multiuser detection, communication signal processing, and smart antennas.

Ta-Sung Lee was born in Taipei, Taiwan, R.O.C., in 1960. He received the B.S. degree form National Taiwan University in 1983, the M.S. degree from the University of Wisconsin, Madison, in 1987, and Ph.D. degree form Purdue University, W. Lafayette, IN, in 1989, all in electrical engineering. In 1990, he joined the Faculty of National Chiao Tung University (NCTU), Hsinchu, Taiwan, where he holds a position as Professor in the Department of Communication Engineering. From 1999 to 2001, he was Director of the Communication and Computer Training Program of NCTU. He is active in research and development in advanced techniques for wireless communications, such as smart antennas for mobile cellular systems, space-time and MIMO transceivers for high data rate transmission, and OFDM based broadband wireless access systems. He has been involved in several National Research Programs, such as the "Program for Promoting Academic Excellence of Universities" supported jointly by the Ministry of Education and National Science Council (NSC) of R.O.C., and the program of "Advanced B3G Radio Access Technologies" supported by the National Telecommunications Program Office. Dr. Lee is a member of Phi Tau Phi Society of R.O.C., and recipient of 1999 Young Electrical Engineer Award of the Chinese Institute of Electrical Engineers and 2001 NCTU Teaching Award.